CHEMICAL PHYSICS

Absolute optical chiral analysis using cavity-enhanced polarimetry

Lykourgos Bougas[1]*, Joseph Byron[2], Dmitry Budker[1,3,4], Jonathan Williams[2,5]

Chiral analysis is central for scientific advancement in the fields of chemistry, biology, and medicine. It is also indispensable in the development and quality control of chiral compounds in the chemical and pharmaceutical industries. Here, we present the concept of absolute optical chiral analysis, as enabled by cavity-enhanced polarimetry, which allows for accurate unambiguous enantiomeric characterization and enantiomeric excess determination of chiral compounds within complex mixtures at trace levels, without the need for calibration, even in the gas phase. Our approach and technology enable the absolute postchromatographic chiral analysis of complex gaseous mixtures, the rapid quality control of complex mixtures containing chiral volatile compounds, and the online in situ observation of chiral volatile emissions from a plant under stress.

INTRODUCTION

Chiral analysis—enantiomeric characterization and enantiomeric excess (e.e.) determination—is a challenging task as the chemical and physical properties of enantiomers are identical, so enantiomers can only be distinguished through their interaction with another chiral object (1). For this reason, analytical techniques such as optical polarimetry, mass spectrometry (MS), and nuclear magnetic resonance (NMR) rely on the chirality of light or of a molecular environment (as in the case of chiral chromatography). These techniques, however, require extensive calibrations for accurate analysis and typically fail to reliably detect chiral compounds at trace levels within complex mixtures. Modern chirality-sensitive optical techniques such as photoionization (2–4), femtosecond (5), microwave (6), and superchiral light–based (7, 8) spectroscopies offer specific advantages, including sensitivities sufficient for gas-phase sensing or the detection of protein monolayers. However, such techniques cannot currently operate within complex environments such as chiral sensing in ambient air. Most crucially, the overall inability of all aforementioned techniques to allow for accurate real-time measurements without the need for calibration prevents in situ real-time study of important chemical, biological, and medical dynamical processes, such as the response of biological organisms to sickness (9) or stress (10).

Molecular optical activity measurements remain the best option to address these limitations. Optical rotary dispersion (ORD) and circular dichroism (CD), in particular, remain the most widely used techniques for measuring chirality (1). However, molecular chiroptical signals are intrinsically weak ($\sim 10^{-5}$ to 10^{-3} rad) and often masked by dominant backgrounds. As a result, the application of chiral analysis by ORD and CD measurements has remained limited to the detection of high-concentration samples, particularly liquids. Recently, a polarimetric technique for enhanced ORD and CD measurements was developed, dubbed as cavity-enhanced chiral polarimetry (CCP) (11–14). CCP uses a ring (four-mirror) optical cavity in a bowtie configuration, where the light always passes

through the chiral sample from the same direction, to enhance the chiroptical signals (ORD and CD) by the large number of cavity passes (optimally $>10^4$; Fig. 1 and fig. S1). Crucially, the placement of an intracavity Faraday rotator, in relation to the symmetry of natural optical activity and the available counterpropagating modes of propagation within the cavity, enables crucial signal-reversal operations that allow for absolute polarimetric measurements not requiring sample removal for a null-sample measurement or instrument calibration (13–15). To date, however, all CCP experiments have used pulse-based measurement approaches [i.e., based on the principles of cavity ring-down polarimetry (13, 14, 16, 17)], which are generally susceptible to detection noise and significant technical noise and result in low numbers of collected photons ($\ll$ milliwatts) and reduced measurement duty cycles (<1%). These are the primary reasons why recent CCP demonstrations have reached only poor chiral detection limits (~microrads per pass) within relatively long integration times (~minutes) (13–15, 18), conditions that have hindered the extension of CCP to real-time chiral analysis. Maximally benefiting from the sensitivity improvement available in a cavity-enhanced approach, as is the case for CCP, becomes feasible in fully continuous-wave measurement schemes. Such schemes require continuous-wave laser sources and application of continuous-wave measurements to enable active control and suppression of technical noise (e.g., vibrational and acoustic noise, thermal drifts), optimal photon collection efficiencies (as high as ~milliwatts) and 100% measurement duty cycles, and the ability to implement high-precision measurement approaches such as optical frequency metrology.

Here, we present the concept of optical-based absolute chiral analysis as enabled by CCP and a measurement approach in which we use a continuous-wave laser source and implement optical frequency metrology (19, 20). Absolute optical chiral analysis allows for (i) absolute enantiomeric identification and direct, accurate determination of the intrinsic specific optical rotation (SOR) of a chiral compound without the need for calibration, (ii) the discrimination of chiral from achiral compounds within complex mixtures and direct estimation of their relevant concentrations, and (iii) absolute e.e. determination. The enhanced signal detection capability offered by CCP allows one to perform these detection capabilities in the gas phase and under a wide range of conditions, such as direct air sampling and/or headspace analysis. The application of optical frequency metrology allows for the continuous measurement of the

[1]Institut für Physik, Johannes Gutenberg-Universität Mainz, Mainz, Germany. [2]Max-Planck-Institut für Chemie, Mainz, Germany. [3]Helmholtz Institute Mainz, GSI Helmholtzzentrum für Schwerionenforschung, Darmstadt, Germany. [4]Department of Physics, University of California, Berkeley, Berkeley, CA, USA. [5]Climate and Atmosphere Research Center, The Cyprus Institute, Nicosia, Cyprus.
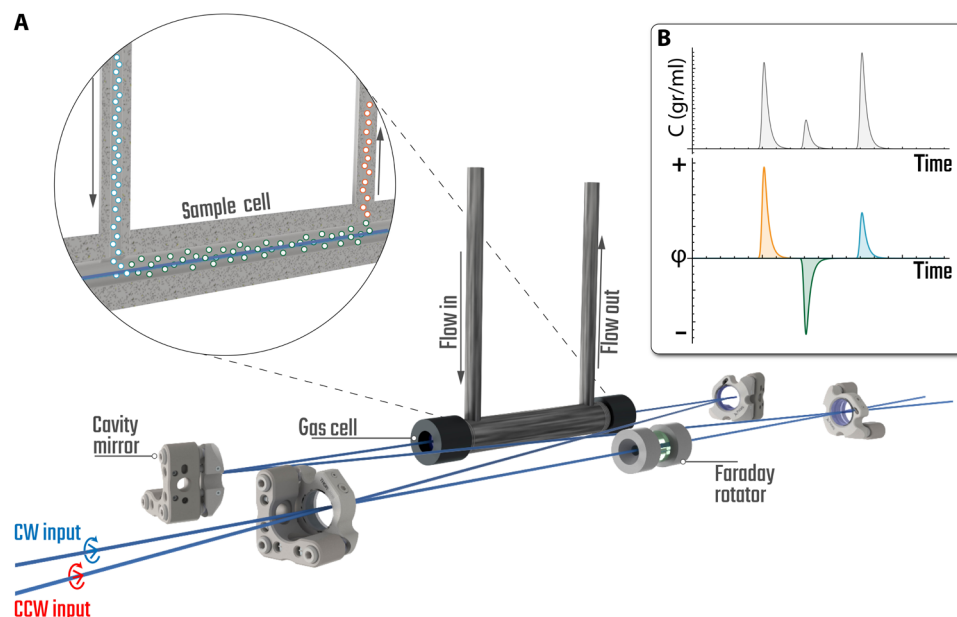*Corresponding author. Email: bougas.lykourgos@gmail.com

Fig. 1. Chiral analysis using CCP. (**A**) Schematic of CCP showing the four mirrors of the optical cavity arranged in a bowtie configuration, the optical beam paths of the allowed counterpropagating laser beams (CW and CCW), the Faraday rotator, and the gas cell. (**B**) The absolute measurement character of CCP allows for direct enantiomer characterization and accurate e.e. determination without the need for calibration via the use of chromatography or a total sample analysis modality.

frequency of the probing radiation as this is referenced, i.e., frequency locked, to the central frequency of a cavity mode [using high-finesse cavities for measurements of linear birefringence, frequency metrology–based approaches have reached ~10^{-13} rad/pass/$\sqrt{Hz}$ detection limits; for an extended analysis, see (*19*) and references therein]. Specifically, for the case of CCP, direct measurement of the frequency difference between the cavity frequency modes of the two available counterpropagating direction modes becomes feasible, which, in turn, enables the absolute measurement of chiral signals (see Materials and Methods). In our case, using a low-finesse cavity (finesse, ~400) and frequency metrology, we are able to reach $\ll 10^{-6}$ rad/pass/$\sqrt{Hz}$ polarimetric, i.e., chiroptical, detection limits, which allow us to extend the application of CCP to the detection of chiral compounds at trace levels in the gas phase in real time. Furthermore, a frequency metrology approach in CCP that relies on the measurement of the central frequency of any cavity mode enables the direct measurement of the average refractive index of the intracavity medium (as cavity resonances depend on the refractive index of the medium). Such a capability becomes critical in accurately quantifying unknown compounds and/or distinguishing chiral from achiral compounds. Overall, using our approach, we demonstrate (i) the absolute chromatographic analysis of complex mixtures in the gas phase without the need for calibration, (ii) the real-time, rapid quality control of complex mixtures containing both chiral and achiral compounds as a means to identify purity or authenticity, and (iii) the in situ monitoring of chiral emissions from a biological organism, a plant, under abiotic, i.e., mechanical, stress.

RESULTS
Gas-phase chiral analysis using GC/CCP
State-of-the-art chiral analysis, especially in the gas phase, is largely performed using MS-based techniques. MS-based chiral analysis

can be realized in combination with different methodic approaches, such as chiral chromatography or chemical reactions with chiral reference molecules (*21*). In all instances, however, extensive calibrations are necessary for accurate quantification of the results and, hence, accurate e.e. determination (i.e., nonabsolute measurement). Furthermore, specifically in the case of using chromatography, the elution order of enantiomers depends on both the chosen column and separation method and can be different for different compounds, which complicates enantiomeric identification.

We demonstrate here how CCP-based absolute chiral analysis overcomes these limitations, specifically by focusing on gaseous samples. In Fig. 2A, we present the specific optical rotatory power $[\alpha]_\lambda^T$ for several gaseous chiral volatile organic compounds (VOCs), particularly monoterpenes [additional data are taken from (*14, 17, 18, 22*)]. In polarimetric-based chiral analysis, the SOR of a substance at a given wavelength can be used to convert the acquired polarimetric signal to concentration. Furthermore, our approach allows us to detect and distinguish between the average refractive index and the chirality parameter of a chiral substance (or even a mixture). Hence, when analyzing complex mixtures that may contain both chiral and achiral compounds, we are able to distinguish these without influencing the quantification of the attainable results. We demonstrate these advantages by combining gas chromatography (GC) with CCP-based chiral detection, i.e., GC/CCP (see also fig. S1). In particular, in Fig. 2B, we show the optical rotation (OR) chromatogram, i.e., φ versus retention time, of a mixture containing several monoterpenes in enantiopure or racemic form. and in Fig. 2C, the OR chromatogram for the case of racemic limonene. In both cases, we can identify the enantiomers of the eluted compounds through the sign of their chiroptical signal, while the refractometric measurements directly reflect their relative concentrations within the prepared mixtures (this feature becomes particularly crucial in the analysis of a compound with unknown specific rotation). Here, gas-phase detection takes place under
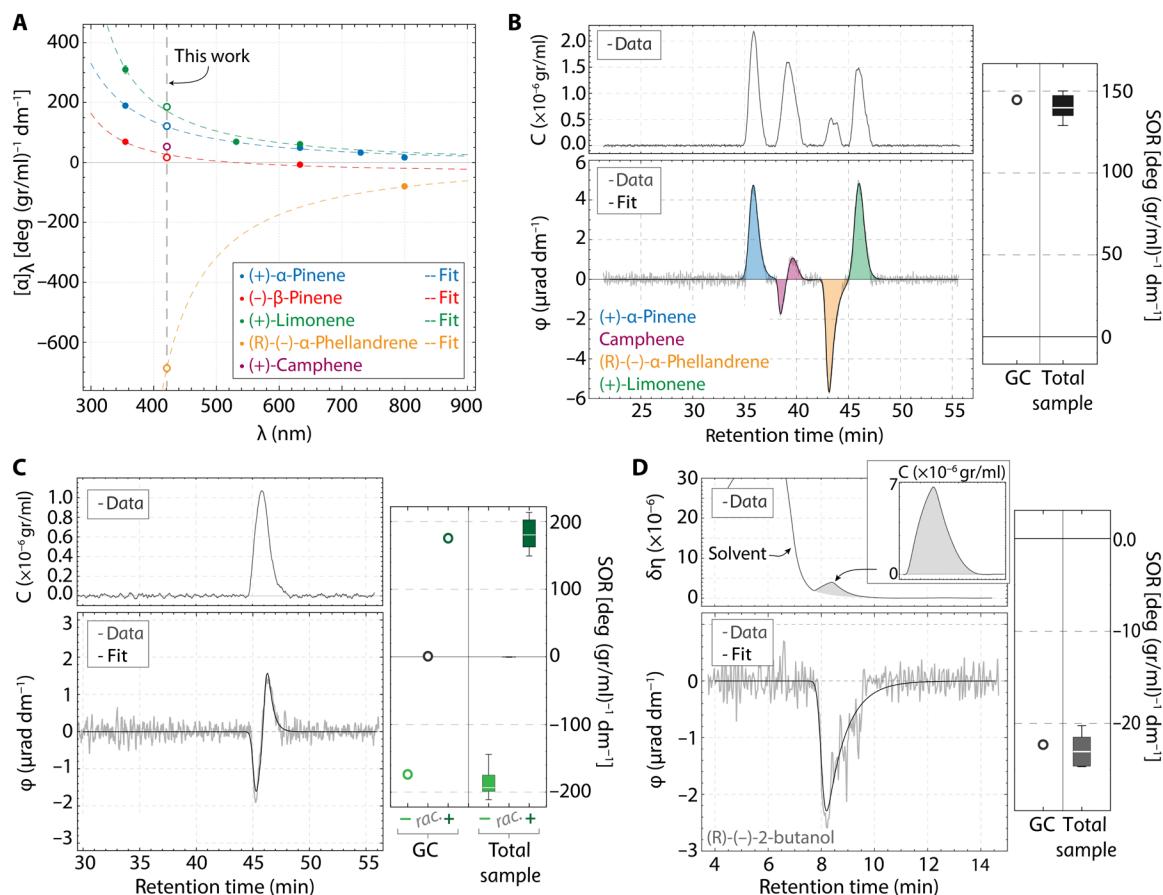
Fig. 2. CCP-based absolute gas-phase chiral analysis using GC and direct total sample measurement. (**A**) Variation of the SOR of different monoterpenes as a function of wavelength, showing our measurements at 421 nm. (**B** to **D**) CCP-based chiral analysis using GC of a mixture of several monoterpenes (B), of racemic limonene (C), and of enantiopure (R)-(−)-2-butanol (D). The OR chromatograms (φ versus retention time) allow for direct enantiomeric characterization and quantitative e.e. determination. The concentration of each analyte is directly extracted through the refractometric measurements [(B) to (D), top] but can also be extracted from the rotation signal (through the SOR). The refractometric measurements also allow us to distinguish achiral and chiral compounds, even when these are coeluting (D). We compare the results obtained from GC/CCP analysis with chirality measurements of the vapors of each mixture, i.e., a total sample analysis, under conditions of direct air sampling. Box-and-whisker plot analysis of total sample chirality measurements (white line represents the mean, and the box height represents 1σ confidence intervals, while the bars represent the maximum and minimum acquired data points). Each box results from the statistical analysis of at least seven measurements performed under ambient conditions using direct air sampling (~20 s of sampling). In all cases, we find our total sample analysis to be in accord with the GC/CCP measurements.

ambient conditions, with the mobile phase being directly expanded into the instrument's intracavity gas cell (Fig. 1) [similar to the operating conditions of GC-olfactometry (*23*)]. For this reason, in conjunction with an incomplete separation, in the case of racemic limonene (Fig. 2C), we observe a single refractometric feature, yet the polarimetric signal allows us to accurately identify the racemic character of the mixture by resolving both enantiomers having equal densities. Crucially, the absolute character of CCP-based detection allows us to accurately and directly infer the elution order of the two enantiomers (in fig. S2, we also present the OR chromatograms for the enantiopure cases). Furthermore, in Fig. 2D, we show the OR chromatogram for the case of enantiopure (R)-(−)-2-butanol. The refractometric signal (δη; Fig. 2D, top) reflects both the solvent and the chiral compound. This allows us to quantify the relative concentration of the target compound within the solution, while the OR signal depends solely on the SOR of (R)-(−)-2-butanol and its concentration. This is in contrast to traditional MS-based detection schemes, where coeluting chiral/achiral compounds are indistinguishable, thus hindering accurate characterization and quantification.

An additional advantage of CCP-based chiral analysis is the ability to perform a total sample analysis via, for instance, dynamic air or headspace sampling (i.e., without using preseparation techniques such as GC; fig. S1). In Fig. 2 (B to D), we compare the GC/CCP results with their respective total sample measurements. Here, these measurements are realized under ambient conditions using dynamic open-air sampling of the chiral vapors of the mixtures prepared for the GC analysis, i.e., without the need for additional sample preparation. In this case, the overall OR signal is equal to the sum of the individual specific rotations from each compound within the mixture times their respective concentrations, which, in turn, relate to their partial pressures ($\varphi_{tot.} = \sum_i c_i \cdot [a]_i$, where $\varphi_{tot.}$ is the measured total OR signal, with c_i and $[a]_i$ being the amount-of-substance faction and SOR, respectively, of each component in the mixture). For the analysis, we normalize the recorded total sample OR signals over their corresponding concentration [as obtained from the refractometric signals (*24*)]. This yields an effective specific rotation for each mixture (in the case of a single compound, such a measurement yields its SOR, $[\alpha]_\lambda^T$; Fig. 2, A to C). We demonstrate

that such a total sample analysis is in accord with the GC/CCP analysis for all examined cases. For the case of single–chiral compound analysis (either within a solution or neat), we find that, as in the case of Fig. 2C where we present the signals for enantiopure (+)/(−)-limonene, this approach allows for direct, rapid e.e. determination. Considering our current polarimetric sensitivity (fig. S1) and the attainable OR signals for the case of, for instance, limonene (Fig. 2, A and C), we can determine gas-phase e.e. at levels better than <1% even under high-noise conditions (dynamic ambient air sampling), within ~1 s of integration time (for the total sample analysis, we present in, e.g., Fig. 2C, the statistical uncertainties originate from the dynamic air sampling).

Real-time quality control via optical chiral analysis

The ability to perform a total sample analysis and measure the overall chiroptical signal of a complex mixture in an absolute manner opens the possibility for accurate quality control analysis in real time. Such a possibility is essential, for instance, in rapidly identifying purity and even authenticity. In the simplest case, a mixture produced using racemates or through chemical synthesis that does not incorporate any enantioselective procedure [e.g., chiral reactants and catalysts (25) or magnetic structures (26)] will be racemic, and hence, its overall OR signal will be zero. In contrast, if such a mixture is produced using natural material sources or enantioselective synthesis, then, in general, it should be chiral, yielding a nonzero OR signal whose sign reflects the chirality of the dominant enantiomers (e.g., Fig. 2, C and D). Furthermore, the ability to simultaneously measure the overall concentration of all volatile (achiral/chiral) components within a complex mixture allows us, in turn, to accurately determine the concentration of the chiral components within it.

An exemplar model of a complex chemical mixture containing both achiral and chiral VOCs is perfume, which typically consists of both natural (originating from essential oils) and synthetic organic compounds. A perfume's quality relies on its fragrance profile, and detailed determination of its composition, i.e., perfume formulation, requires analytical techniques such as GC/MS. This becomes particularly complex in analytical quality control, considering that perfumes consist of several hundreds or even thousands of different compounds. Notwithstanding, chemical fingerprinting can also be used for quality control, which can enable rapid, real-time quality analysis, becoming, in turn, vital in identifying, for instance, counterfeit perfumes.

We demonstrate here how absolute optical chiral analysis can be used for the (rapid) quality control of perfumes directly in the gas phase without any sample preparation (e.g., possible via dynamic air sampling through nebulizing from the original bottle). By measuring the overall chiroptical signal of a perfume, we obtain a distinct dynamic chiral signature rather than a multicomponent spectrum as in the case of MS-based schemes, i.e., chiral fingerprinting. For our demonstrations, we use four authentic perfumes (eau de parfum): "Coco Mademoiselle" ("CM") by Chanel, "Miss Dior" ("MD") by Dior, "Angel" by Thierry Mugler, and "La vie est belle" ("LVeB") by Lancôme. As model counterfeit/adulterated samples, we use their, commercially available, low-cost fragrance clones (see Materials and Methods for an extensive list). Low-cost clones also contain compounds originating from natural or enantiopure sources and are thus particularly suitable for a quantitative quality comparison (a fully synthetic perfume, where any chiral molecule would be present in racemic form, will yield a null chiroptical signal). In

Fig. 3A, we show a real-time comparison between the observed ambient signal for an authentic perfume (CM) and that for one of its low-cost clones, in which the authentic perfume yields a positive chiral signal, whereas the clone yields a null signal. GC/MS analysis reveals that the observed differences in the chiral OR signals cannot be attributed to a single component but to an overall difference in compositions [e.g., (−)-β-pinene is the dominant component in the low-cost alternative versus (+)-limonene in the authentic perfume; Fig. 3B]. GC/MS analysis allow us to corroborate the positive chiral character of the authentic perfume, attributed to (+)-limonene, which is the dominant monoterpene in most citrus-based essential oils (27). The observed null signal for the fragrance clone (AC#1; Fig. 3A), however, indicates that any chiral substances present within its matrix (Fig. 3B) are at much lower concentrations than in the authentic perfume and, in this case, at concentrations lower than our current detection limits. In addition, the refractometric signals, largely dominated by the alcohols that have the highest concentration (70 to 80%) within the perfumes, allow us to record distinct differences between the matrices of the two perfumes, assisting identification (Fig. 3A). Using both refractometric and chirality measurements, we present in Fig. 3 (C and D) an overall comparison between the chiral signatures of several authentic perfumes with their respective low-cost fragrance clones. We also perform measurements on samples from different (purchased) bottles for each of the authentic perfumes to establish the validity of our approach toward quality control. We observe similar chiroptical signals for the same perfume from different packages. Overall, we demonstrate that we can accurately, and in a quantitative manner, distinguish high-quality perfumes from each other and from their low-cost clones using their chiroptical signatures, as these originate from differences in their composition and even possible adulteration. In particular, for the case of the authentic CM and MD, the similarities between their monoterpene chromatograms (fig. S3) suggest that considerable analysis using, for instance, chiral GC/MS is required to accurately distinguish them. In contrast, absolute optical chiral analysis enables us to distinguish between them directly in a rapid single measurement using their distinct chiral signatures.

Online in situ chiral analysis of VOC emissions from biological organisms

Real-time absolute chiral analysis in the gas phase opens up the possibility for observing in situ the emissions of chiral VOCs from biological organisms such as plants. An estimated ~760 Tg (C) of biogenic VOCs (BVOCs) enters Earth's atmosphere every year primarily from terrestrial vegetation (28) [contributing also to the production of secondary organic aerosols that affect Earth's radiative budget (29)]. BVOC emissions are the result of the biological functions of plants, i.e., their metabolism and response mechanisms, and serve as the plant's main communication and interaction channel with the surrounding environment (10). Specifically, plants release BVOCs into the surrounding air in response to both abiotic (e.g., light or soil conditions) and biotic (e.g., herbivores or pests) stress factors (30). Monoterpenes are among the most abundant BVOC species observed in the atmosphere (~11%) (28), many of which are chiral and naturally exist as enantiomeric pairs in the atmosphere at mixing ratios of ≲ parts-per-billion by volume (ppbv) (31, 32). However, their chiral nature is largely ignored in air-chemistry studies and related models (28), as their enantiomers are not quantified separately and are modeled as having similar source
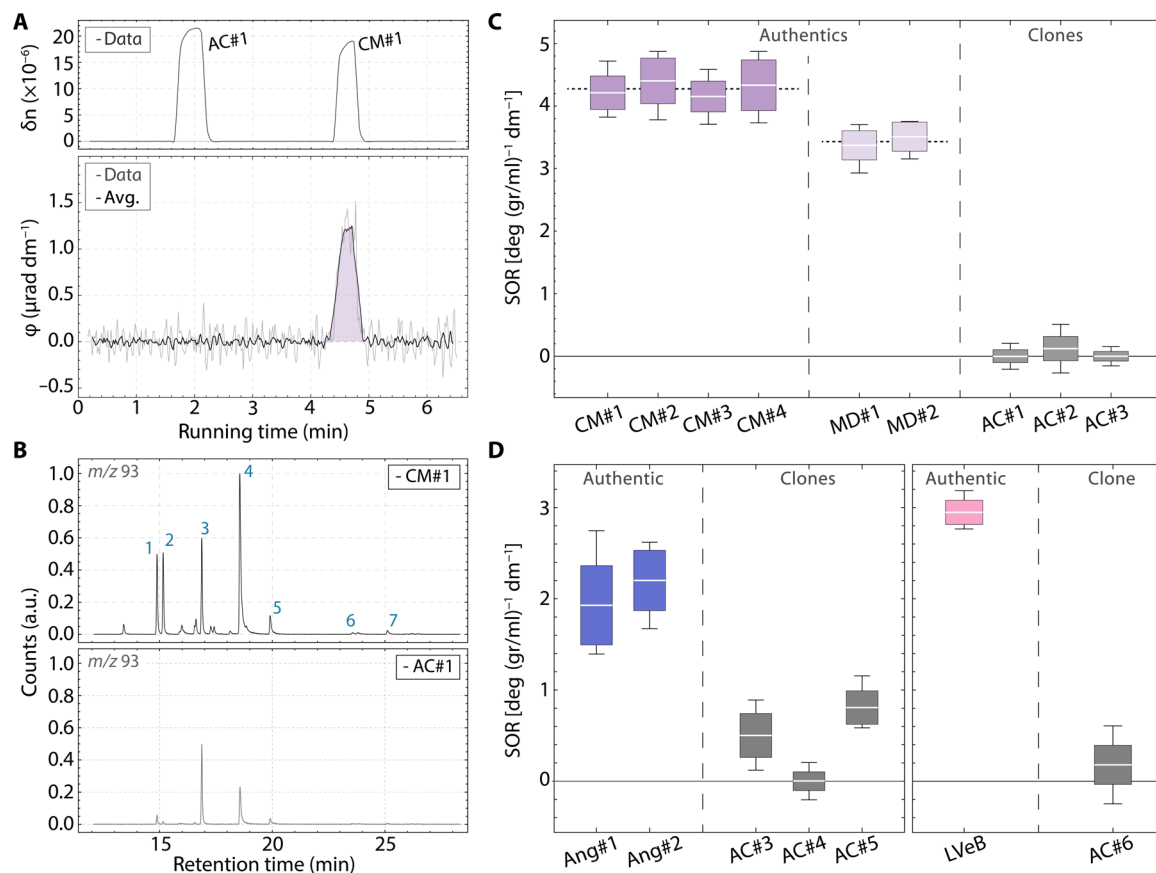
Fig. 3. Perfume quality control using CCP-based absolute chiral analysis. (**A**) Real-time CCP measurements of an authentic perfume (CM by Chanel) versus one of its low-cost fragrance clones (AC#1), under conditions of direct ambient-air sampling (fig. S1). Time separation between measurement points is 0.5 s (i.e., equal to the integration time for each measurement). (**B**) GC/MS chromatograms of CM (CM#1) and of AC#1 revealing the following dominant chiral volatile compounds: 1, (−)-α-pinene; 2, (+)-α-pinene; 3, (−)-β-pinene; 4, (+)-limonene; 5, γ-terpinene; 6, (−)-linalool followed by (+) linalool; and 7, linalyl acetate. (**C** and **D**) Box-and-whisker plot analysis comparison of chiroptical measurements for different authentic perfumes (CM, MD, Ang, and LVeB; see Materials and Methods for details) versus their respective low-cost alternatives. The white lines represent the mean, and the box heights represent 1σ confidence intervals, while the bars represent the maximum and minimum acquired data points. Each box results from the statistical analysis of at least seven measurements performed under ambient conditions using dynamic air sampling (~20 s of sampling). Overall, absolute chiral analysis allows for accurate, quantitative quality control of authentic perfumes while enabling the rapid identification of a perfume imitation. *m/z*, mass/charge ratio; a.u., arbitrary units.

characteristics, based on their identical physical properties (boiling point and exact mass) and observed reaction rates with oxidants. Similarly, studies of BVOC emissions from individual plants largely ignore their chiral nature, despite the fact that chiral chemodiversity within a plant's VOC emission profile has a critical role both in (mutually benefiting) plant-insect (*33*) and plant-plant (*34*) interactions.

Recent air-chemistry studies have revealed puzzling effects that stress the need to investigate the role of chirality in BVOC emissions. These unexpected effects are (i) regiospecific behavior in the enantiomers of BVOCs, such as α-pinene (*35*); (ii) diurnal enantiospecific enhancements in BVOC emissions in boreal forests (*36, 37*); (iii) enantiospecific compositional changes of BVOCs over the Amazon forest as a function of altitude, time, and season (*32*); and (iv) compartment enantiospecific emissions identified in coniferous trees (*38*). These findings reveal gaps in our understanding of how emissions are controlled and modeled (*28, 39*), particularly considering that processes in the atmosphere such as photooxidation are not expected to be enantioselective, whereas microbial degradation (*40*) and plant metabolism (*10*) are. Air-chemistry studies are, almost in

their entirety, realized using MS-based analysis, which requires chiral GC to quantify enantiomers separately. Such studies, therefore, typically require on-site sampling that leads to poor time resolutions (samples are typically collected every ~2 to 3 hours) (*32, 37, 38*) and often difficult-to-predict uncertainties during offline analysis (*41, 42*).

Here, we measure the chirality of the volatile emissions of a plant under mechanical wounding, in situ. The principal motivation for such a measurement is the initiation of a thorough investigation on mechanical damage as a stress mechanism responsible for the observed chiral composition changes of VOCs over different ecosystems, such as boreal forests (*43, 44*) and the Amazon rainforest (*32*). Here, we use a coniferous plant, *Pinus heldreichii* (Fig. 4A), and record the chiral dynamics of its branch emissions following mechanical wounding, i.e., the complete cut of one of the branches of the plant. Not only for comparison but also as validation of our approach with state-of-the-art techniques used in similar studies, we use together with our online CCP-based measurements an offline chiral GC/MS–based analysis.

We first measure the plant emissions for several hours before wounding to establish a baseline for their overall concentration and chiral OR signal with our online CCP measurement. Using the offline GC/MS analysis, we are additionally able to establish the compositional character of the branch emissions (sampling times for the online and offline measurements are 15 and 10 min, respectively). In the resting state, the dominant chiral VOCs in the plant emissions are monoterpenes that primarily originate from de novo synthesis and evaporation from storage structures (45, 46). The CCP-based measurements reveal an overall concentration of the emitted monoterpenes at the ~1 part-per-million by volume (ppmv) levels and a negative chiral OR signal (Fig. 4, B to D). The offline GC/MS analysis allows us to specifically identify (±)-α-pinene, (±)-camphene, (−)-β-pinene, and (±)-limonene as the principal monoterpene VOCs in the plant emissions and to corroborate the concentration measurement of the plant emissions with our CCP measurements (Fig. 4E). In addition, from the GC spectra, we observe that (−)-limonene dominates the overall emission profile,

thus confirming the overall recorded negative OR signal, while we see that the (+)-α-pinene isomer prevails over its (−)-isomer.

Following mechanical wounding, we observe an abrupt ~10-fold increase in the concentration of the plant emissions that drop with a characteristic time of ~4 hours to stabilize at densities approaching their prewounding values, in accordance with similar observations in the literature (47). Such a dynamical behavior is established by both online and offline measurements (Fig. 4C). The chiroptical OR signal (Fig. 4D), however, becomes more negative to reach a maximal negative value within ~6 hours from the wounding [approaching the specific rotation value for enantiopure (−)-limonene; see Fig. 2A] while stabilizing long term to an OR signal value that is more negative than its initial (before wounding) resting one. The observation of such a distinct difference between the dynamics in the chiroptical OR signal and those of the overall VOC concentration signal directly reveals the presence of chirally specific differences in the dynamic behavior of different monoterpene isomers and their respective enantiomers. Specifically, our refractometric measurements (Fig. 4B
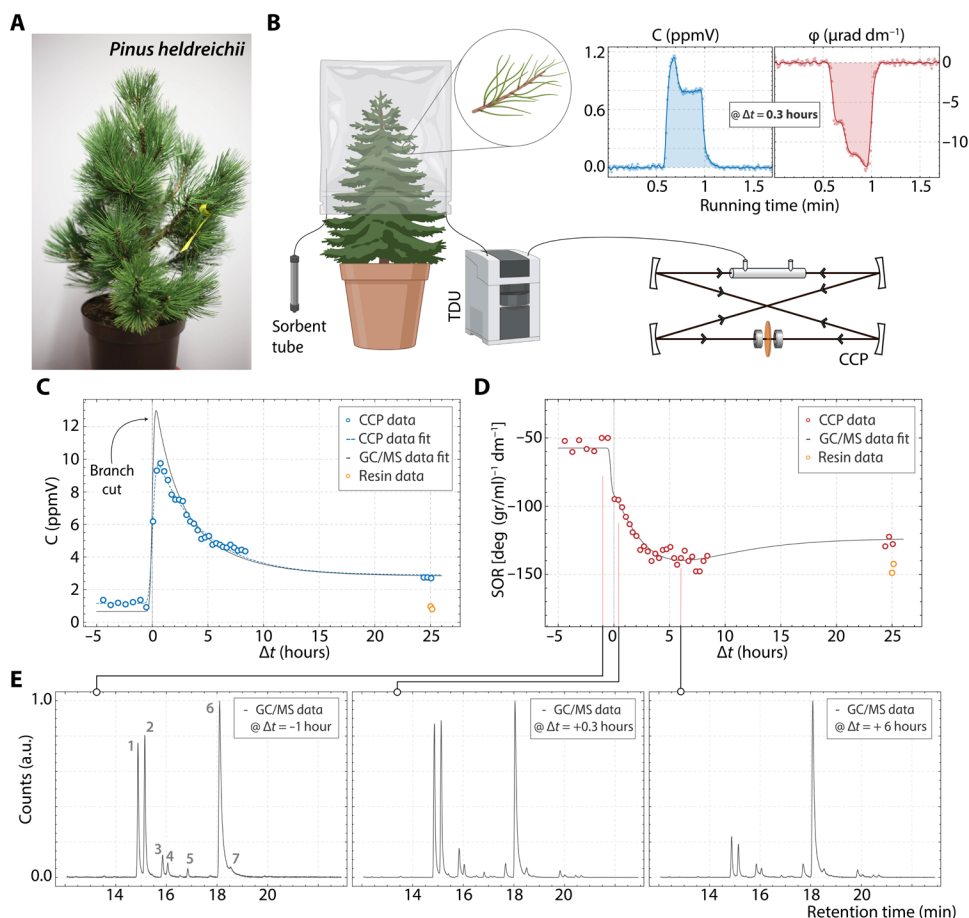

Fig. 4. Online in situ chirality measurements of the emissions of a coniferous plant during mechanical wounding. (**A**) Photo of the coniferous plant used in the measurements, *P. heldreichii*. (**B**) Schematic of the setup required to sample and measure the chirality of the VOC emissions from the branches of the plant (before and after wounding) using CCP (TDU). Sorbent tubes are required for the offline chiral GC/MS analysis. Insets show postwounding CCP measurements revealing the presence of different compounds in the emissions and an overall negative OR signal. (**C** and **D**) Concentration (as obtained through refractometric measurements and corroborated via GC/MS analysis) and OR signals (normalized over concentration). Yellow points correspond to concentration and chirality measurements from the secreted resin that covers the wounding site. (**E**) GC/MS chromatograms for different times before and after wounding. The spectra are normalized over their respective signal value for (−)-limonene (peak 6) to visually aid the comparison between the relative signal changes among all eluted compounds. Labeled peaks: 1, (−)-α-pinene; 2, (+)-α-pinene; 3, (−)-camphene; 4, (+)-camphene; 5, (−)-β-pinene; 6, (−)-limonene; 7, (+)-limonene.

and fig. S9), corroborated by the GC/MS analysis (Fig. 4E and fig. S8), allow us to identify that the observed chiral dynamics, toward more negative values, are the result of the dominance of (−)-limonene in the overall emission profile and of a relative increase in the (−)-α-pinene enantiomer over its (+)-enantiomer [which, in turn, is in accord with observations from other studies and in line with the results obtained from the relevant Amazon measurements (32)]. To provide further insight into the observed chiroptical signals, we independently record also the chiral OR signal from the resin secreted by the plant's storage ducts that eventually hardens to seal the wound site (fig. S10). The long-term recorded OR signal value of the plant emissions is close to the OR signal value obtained independently from the resin (Fig. 4, C and D), indicating that chiral VOC composition of the resin dominates the overall emission profile of the plant in the long-term, following mechanical wounding.

DISCUSSION
Optical-based technologies hold the potential for surpassing critical limitations in current state-of-the-art techniques used for chiral analysis, such as MS and NMR. We demonstrate how continuous-wave cavity-enhanced optical polarimetry, specifically CCP through the implementation of a frequency metrology measurement scheme, enables real-time chiral analysis of complex chemical mixtures in an absolute manner, i.e., without the need for calibration, at trace quantities (e.g., gas phase).

Specifically, we first demonstrate the CCP-based absolute chiral analysis of gaseous mixtures using GC. Our current instrument sensitivity is ~3.4×10^{-7} rad/√Hz (20 μdeg within 0.5 s of integration time) and is ultimately limited by photon shot noise at the 1.3×10^{-9} rad/√Hz level (fig. S1). Considering the typical values for the SOR of monoterpenes [~100 deg (gr/ml)$^{-1}$ dm^{-1}; Fig. 2A], such limits correspond, respectively, to gas sensitivities of ~35 ppmv/√Hz and ~131 ppbv/√Hz. Instrument and technique improvements, however, which may include the use of a higher-finesse optical cavity, higher-quality intracavity optics, and alternative detection schemes, can lead to chiroptical sensitivities of ~10^{-13} rad/√Hz (19, 20), which correspond to concentration sensitivities of <10 pptv/√Hz. Such sensitivities match those attainable with current state-of-the-art MS-based detection methodologies.

Second, we demonstrate rapid analysis of complex chemical mixtures containing both chiral and achiral compounds using their distinct gas-phase chiral signatures. As our target system, we select perfume, complex mixtures that contain both achiral and chiral compounds. Accurate, quantitative component analysis of perfumes is typically performed using GC/MS, which, for routine quality controls in the perfume industry and in security areas, is undesirably slow and requires calibration. Alternative approaches, such as variants of ambient MS [e.g., electrospray ionization MS (48, 49)], do not demand chemical derivatization or chromatographic separation but require either liquid samples, a surface infused with the perfume (i.e., paper strip), or elaborate sample preparations. Overall, MS-based approaches typically require integration times of several seconds to minutes to achieve optimum sensitivities and the implementation of background subtraction procedures for quantitative results (i.e., nonabsolute) (48, 49). Furthermore, the principal ingredients for (high-quality) perfumes are essential oils and organic synthetic aroma compounds. Essential oils, in particular, originate from natural sources, most typically plants, and therefore are generally chiral. They are also primary materials for the flavor, health, and agriculture industries. Our approach that includes no sample preparation and the ability for rapid trace chiral analysis can be implemented for quality control (authentication and detecting adulteration) in all aforementioned commercial applications, including also the analysis of drugs, which largely consist of chiral compounds.

Third, we demonstrate online real-time chiral analysis of VOCs emitted by a biological organism under stress, in this case a coniferous plant. The scientific challenge for modern atmospheric organic chemistry is to identify all available BVOC sources and the physical and chemical processes determining the fate of volatile compounds, for a deeper understanding of their overall impact on atmosphere and climate (39). To do so, accurate in situ real-time measurements of the short- and long-term dynamics of BVOCs are necessary, and the chirality of the compounds has to become an integral aspect of the active research, as their chirally specific dynamics (i.e., enantiospecific dynamics of different compounds; see Fig. 4, C and D) can serve as a unique signature for hitherto uncharacterized BVOC sources. Here, we show how observations of chiral emissions from a coniferous plant following mechanical wounding can allow us to observe the enantiospecific dynamics of different compounds stored within the plant and even the resin that seals the wounding site. Such measurements are valuable in identifying, in situ and in real time, abiotic from biotic stress factors (30) and the underlying enzyme-driven response mechanisms (50). Damage to boreal forests by bark-boring beetles generates chiral signals similar to those of mechanical stress [i.e., strong increase in (+) enantiomers] and recent observations in the Amazon forest of unusual enantiospecific changes of chiral BVOCs that have been attributed to insect proliferation (32). Most crucially, real-time chiral analysis of VOCs emitted by plants can also enable the noninvasive health status monitoring of plants and crops, contrary to the invasive electrophysiological measurements. Furthermore, the absolute optical chiral analysis approach and technique that we present in this work can enable in situ real-time observations of the role of chirality in the oxidation products of chiral BVOCs, which, in turn, contribute to the production of secondary organic aerosol particles (51, 52). Therefore, our approach can allow for novel insights into not only the formation but also transformation processes of atmospheric aerosols and assist in determining their climate-relevant properties, as in the case of, e.g., establishing a link between molecular chirality and cloud activation potential of secondary organic aerosol particles (53, 54).

Numerous additional scientific and commercial applications can benefit from our approach, specifically concerning gas-phase chiral analysis. One prominent example is in the search of chirality and potential chiral asymmetries on celestial bodies (planets and comets) as a sign of life, where traditional chiral-sensing technologies such as chiral GC/MS [e.g., the European Space Agency's ROSETTA mission (55)] are currently used. The inability to provide accurate, quantitative results without calibration is vital for such searches, and our approach can resolve these limitations. Last, the concept of absolute chiral analysis can be extended to the nanoscale using recent developments in nanophotonic/plasmonic-based chirality-sensitive schemes (56, 57). Such a possibility can enable the real-time in situ investigation of chiral dynamics in the nanoscale such as the investigation of protein dynamics in situ. Nanophotonic approaches open the possibility for ultraminiaturized systems of low-cost and low-energy consumptions suitable for lab-on-a-chip devices.

MATERIALS AND METHODS
Experiment
For all experiments presented in this work, we use an external cavity diode laser with a center wavelength of $\lambda = 421$ nm (Toptica DL-PRO). The CCP device we use consists of a ring (four-mirror) optical cavity with the mirrors arranged in a bowtie configuration (Fig. 1 and fig. S1) (*11–14*). Such an optical cavity supports two distinct counterpropagating laser beams, which we denote as clockwise (CW) and counterclockwise (CCW) (according to their propagation within the cavity). The optical cavity has a total length of $L = 1.17$ m and consists of highly reflective concave mirrors with radii of curvature of 1 m (FiveNine Optics; specified reflectivity $R \sim 99.9\%$ at 421 nm). A gas cell is positioned on one arm of the optical cavity and consists of a steel cylinder with a length of $l = 10$ cm and an inner volume of 1.2 ml. Two anti-reflection- (AR-)–coated SiO_2 windows (FiveNine Optics; AR coated with specified $R < 0.01\%$ per surface) are used to seal the gas cell. Under this configuration, the optical finesse of the cavity is $\mathcal{F} \approx 400$. Gaseous mixtures (chiral vapors) are introduced into the gas cell via PEEK (polyether ether ketone) tubing. We use a 6.35-mm-thick AR-coated SiO_2 window as an intracavity magneto-optic crystal to generate Faraday-related circular birefringence, θ_F, with the use of permanent magnets attached directly to the mount holder of the substrate (in our case, we obtain $\theta_F \approx 2°$) (*58*). This intracavity Faraday rotation symmetrically splits the cavity resonances into two (orthogonal) circularly polarized cavity modes, i.e., one resonant for right circularly polarized light and the other for left circularly polarized light and hence denoted hereafter as R and L modes. The resulting R-L cavity modes are separated by $2f_F = 2\theta_F \cdot \frac{FSR}{\pi}$, where $FSR = \frac{c}{nL}$ is the cavity's free spectral range, c is the speed of light, L is the length of the cavity, and n is the refractive index of the intracavity medium. In our experiments, we obtain $f_F \approx 2.8$ MHz. The intracavity Faraday circular birefringence also suppresses the effects of any possible intracavity linear birefringence (*11–14*), ensuring the conservation of the circular polarization character of the R-L modes. In the absence of any chiral substance, the R-L mode frequency splitting is identical for both CW and CCW propagation directions. The introduction of a chiral substance causes circular birefringence (φ_c), which causes the frequency splitting between the R and L modes to be different for the CW and CCW propagation directions, i.e., $\delta f_{CW} = 2 |f_F + f_c|$ and $\delta f_{CCW} = 2 |f_F - f_c|$, where $f_c = \varphi_c \cdot \frac{FSR}{\pi}$. Thus, the cavity-mode (frequency) spectrum consists of four distinct (nondegenerate) modes, R_{CW}, L_{CW}, R_{CCW}, and L_{CCW}, which enables us to determine φ_c by directly measuring f_c (fig. S1). Measurement of the average refractive index, n_c, becomes possible through the direct measurement of the central frequencies of any of the cavity modes. To do so accurately, we servo-lock the emission frequency of the laser to a cavity resonance (in our experiments, either R_{CW} or L_{CW}). In this case, the laser wavelength is fixed, while its frequency tracks the changes in refractive index, since $\delta f/f = -\delta n/n$. From the gas refractivity measurements, we can then extract the density of the compound under investigation (*24*).

GC/CCP analysis
In all cases of GC/CCP analysis, we use splitless injection (Agilent HP 6890A GC, Agilent Technologies, USA) of mixture solutions in ethanol (1 μl of solution injected). The chiral separations of the monoterpene mixture (Fig. 2B) and racemic limonene (Fig. 2C) were achieved using a 120-m β-DEX 120 column (Sigma-Aldrich GmbH, Germany) with 0.25-mm internal diameter and 0.25-μm film thickness. The column flow was chosen to be 1.5 ml/min and the temperature program to be 40°C for 4 min then 40° to 110°C at 3.5°C min^{-1}, 20 min at 110°C (isothermal), and 110° to 210°C at 10°C min^{-1}. For the OR chromatogram of (R)-(−)-2-butanol (Fig. 2D), we used a 60-m β-DEX 120 column (Sigma-Aldrich GmbH, Germany) with 0.25-mm internal diameter and 0.25-μm film thickness. The column flow was chosen to be 2.5 ml/min and the temperature program to be 40°C for 4 min then 40° to 100°C at 5°C min^{-1} and 100° to 210°C at 30°C min^{-1}. For the mixtures, we use enantiopure (+)-α-pinene, (+)-α-pinene, (R)-(−)-α-phellandrene, (+)-limonene, (−)-limonene, (R)-(−)-2-butanol, and racemic camphene (all compounds purchased from Sigma-Aldrich). For the measurements shown in Fig. 2B, we prepare the following mixture: 120 μl of (+)-α-pinene, 100 μl of camphene, 20 μl of (R)-(−)-α-phellandrene, and 90 μl of (+)-limonene.

CCP-based chiral analysis of perfumes
All perfumes were purchased from local retail stores. The low-cost fragrance clones that we use for quality comparison with the authentic ones are as follows: "Suddenly Madame Glamour" by Lidl (AC#1), "Magic" by Miro (AC#2), and "Madame Isabelle" by La Rive (AC#3) as alternatives for CM by Chanel and MD by Dior; "River of Love" by La Rive (AC#4), "Wish" by Chopard (AC#4), and "Diable Bleu" by Creation Lamis (AC#5) as alternatives for Angel by Thierry Mugler; and "Queen of Life" by La Rive (**AC#6**) as the alternative for LVeB by Lancôme. All perfume measurements are realized using dynamic air sampling with the help of a pump and a flow controller (Bronkhorst F-201CV) that allows us to control and keep constant the sampling flow (sampling flow rates of ~30 ml/min were used for the measurements). For the sampling and transfer lines, we use PEEK tubing (inner diameter of 0.74 mm, Supelco Inc.).

CCP-based chiral analysis of chiral emissions from a plant
The *P. heldreichii* that we use for our measurements was purchased from a local greenhouse (Blumenhaus Smedla, Mainz, Germany) and has a total height of ~80 cm (Fig. 4A). We use a 25-liter Tedlar sampling bag (ANALYT-MTC GmbH, Germany) secured around the tree stem to create an open-bottom sampling chamber that encloses the plant's upper branches (Fig. 4B; icons created with BioRender.com). This open-bottom design allows air to move between the interior and exterior of the enclosed space to avoid possible suffocation of the plant during sampling (we do not implement any active mixing of both air volumes), while we ensure that the sampling volume is located at a significant distance from the plant's soil (>10 cm) to avoid signal contamination from the soil compartment. A heating tape supported around the sampling bag allows us to actively control the temperature within the sampling chamber (during the measurements, we continuously monitor and keep stable the temperature within the sampling chamber; see fig. S6). We ensure that the heating tape is not in contact with either the branches or the needles of the plant to avoid any contribution to the signal originating from possible local heat-induced damage. For the continuous online sampling, we use a thermal desorption unit (TDU; TT24-7 x-r, Markes International), and we sample ~1 liter of ambient air from the chamber through the bag's valve. Using helium 6.0 as the carrier gas, we transfer the desorbed sample through PEEK tubing (inner diameter of 0.5 mm, Supelco Inc.) to the intracavity gas cell for the CCP-based chirality measurements.

Offline chiral analysis using GC/MS

For the offline GC/MS analyses presented in this work, we proceed as follows: For the perfume analysis, we fill scintillation vials (20 ml) with ~0.2 ml of perfume and use passive headspace sampling into sorbent tubes (typical exposure time, ~15 s). To sample the pine plant emissions, we use a 6.35 mm Teflon sampling line placed inside the sampling bag, to which the sorbent tubes are connected, outside the bag; samples are collected onto the sorbent cartridges at 200 ml/min for ~10 min using a GilAir Plus Personal Air Sampling Pump (Sensidyne, USA). The sorbent cartridges, used in both cases, are made from inert-coated stainless steel (SilcoNert 2000, SilcoTek, Germany), and the sorbent consists of 150 mg of Tenax TA followed by 150 mg of Carbograph 5 TD ($560 \ m^2/g$). The size of the Carbograph particles is in the range of 20 to 40 mesh. The Carbograph 5 was supplied by L.A.R.A s.r.l. (Rome, Italy) and the Tenax by Buchem BV (Apeldoorn, The Netherlands). The cartridges are desorbed using a TD100-xr automated TDU (Markes International Ltd., UK). The cartridges are first dry purged at 50 ml/min of helium 6.0 carrier gas for 5 min to remove water before being desorbed with a flow of 50 ml/min at 250°C for 10 min. After cartridge desorption, the sample is transferred to the cold focusing trap (material emissions cold trap, Markes International, UK) at 30°C. The trap is purged at 50 ml/min of helium 6.0 carrier gas for 1 min and is then desorbed at 250°C for 3 min. Specifically, for the measurements of the pine plant emissions, cartridges that are sampled before the pine tree branch was broken are desorbed with a split ratio of 221:1, whereas cartridges that are sampled after the branch breaking were desorbed with a split ratio of 1005:1. In all cases, the sample matrix was separated and detected using a GC/TOF-MS (GC 7890B, Agilent Technologies, USA; BenchToF-select, Markes International Ltd., UK). The chiral separation is achieved using a 30-m β-DEX 120 column (Sigma-Aldrich GmbH, Germany) with 0.25-mm internal diameter and 0.25-μm film thickness. The column flow is chosen to be 1 ml/min and the temperature program to be 40°C for 5 min then 40° to 150°C at 4°C min^{-1} until 220°C and then held again for 5 min. Identification of the target compounds was achieved by comparing the obtained mass spectra to the National Institute of Standards and Technology database library and by spiking clean cartridges with the headspace from the relevant liquid standard. Each target compound was calibrated separately at each split ratio using a gas standard mixture (Apel-Riemer Environmental Inc., 2019) and liquid standards of chiral molecules.

SUPPLEMENTARY MATERIALS
Supplementary material for this article is available at https://science.org/doi/10.1126/sciadv.abm3749

REFERENCES AND NOTES

1. P. L. Polavarapu, *Chiral Analysis: Advances in Spectroscopy, Chromatography and Emerging Methods* (Elsevier Science, ed. 2, 2018).
2. M. H. M. Janssen, I. Powis, Detecting chirality in molecules by imaging photoelectron circular dichroism. *Phys. Chem. Chem. Phys.* **16**, 856–871 (2014).
3. M. Pitzer, M. Kunitski, A. S. Johnson, T. Jahnke, H. Sann, F. Sturm, L. P. H. Schmidt, H. Schmidt-Böcking, R. Dörner, J. Stohner, J. Kiedrowski, M. Reggelin, S. Marquardt, A. Schießer, R. Berger, M. S. Schöffler, Direct determination of absolute molecular stereochemistry in gas phase by Coulomb explosion imaging. *Science* **341**, 1096–1100 (2013).
4. A. Comby, E. Bloch, C. M. M. Bond, D. Descamps, J. Miles, S. Petit, S. Rozen, J. B. Greenwood, V. Blanchet, Y. Mairesse, Real-time determination of enantiomeric and isomeric content using photoelectron elliptical dichroism. *Nat. Commun.* **9**, 5212 (2018).
5. H. Rhee, Y.-G. June, J.-S. Lee, K.-K. Lee, J.-H. Ha, Z. H. Kim, S.-J. Jeon, M. Cho, Femtosecond characterization of vibrational optical activity of chiral molecules. *Nature* **458**, 310–313 (2009).
6. D. Patterson, M. Schnell, J. M. Doyle, Enantiomer-specific detection of chiral molecules via microwave spectroscopy. *Nature* **497**, 475–477 (2013).
7. Y. Tang, A. E. Cohen, Enhanced enantioselectivity in excitation of chiral molecules by superchiral light. *Science* **332**, 333–336 (2011).
8. E. Hendry, T. Carpy, J. Johnston, M. Popland, R. V. Mikhaylovskiy, A. J. Lapthorn, S. M. Kelly, L. D. Barron, N. Gadegaard, M. Kadodwala, Ultrasensitive detection and characterization of biomolecules using superchiral fields. *Nat. Nanotechnol.* **5**, 783–787 (2010).
9. A. W. Boots, J. J. B. N. van Berkel, J. W. Dallinga, A. Smolinska, E. F. Wouters, F. J. van Schooten, The versatile use of exhaled volatile organic compounds in human health and disease. *J. Breath Res.* **6**, 027108 (2012).
10. N. Dudareva, F. Negre, D. A. Nagegowda, I. Orlova, Plant volatiles: Recent advances and future perspectives. *Crit. Rev. Plant Sci.* **25**, 417–440 (2006).
11. L. Bougas, G. E. Katsoprinakis, W. von Klitzing, J. Sapirstein, T. P. Rakitzis, Cavity-enhanced parity-nonconserving optical rotation in metastable Xe and Hg. *Phys. Rev. Lett.* **108**, 210801 (2012).
12. L. Bougas, G. E. Katsoprinakis, W. von Klitzing, T. P. Rakitzis, Fundamentals of cavity-enhanced polarimetry for parity-nonconserving optical rotation measurements: Application to Xe, Hg, and I. *Phys. Rev. A* **89**, 52127 (2014).
13. D. Sofikitis, L. Bougas, G. E. Katsoprinakis, A. K. Spiliotis, B. Loppinet, T. P. Rakitzis, Evanescent-wave and ambient chiral sensing by signal-reversing cavity ringdown polarimetry. *Nature* **514**, 76–79 (2014).
14. L. Bougas, D. Sofikitis, G. E. Katsoprinakis, A. K. Spiliotis, P. Tzallas, B. Loppinet, T. P. Rakitzis, Chiral cavity ring down polarimetry: Chirality and magnetometry measurements using signal reversals. *J. Chem. Phys.* **143**, 104202 (2015).
15. D.-B.-A. Tran, K. M. Manfred, R. Peverall, G. A. D. Ritchie, Continuous-wave cavity-enhanced polarimetry for optical rotation measurement of chiral molecules. *Anal. Chem.* **93**, 5403–5411 (2021).
16. T. Müller, K. B. Wiberg, P. H. Vaccaro, Cavity ring-down polarimetry (CRDP): A new scheme for probing circular birefringence and circular dichroism in the gas phase. *J. Phys. Chem. A* **104**, 5959–5968 (2000).
17. T. Müller, K. B. Wiberg, P. H. Vaccaro, J. R. Cheeseman, M. J. Frisch, Cavity ring-down polarimetry (CRDP): Theoretical and experimental characterization. *J. Opt. Soc. Am. B* **19**, 125–141 (2002).
18. A. K. Spiliotis, M. Xygkis, E. Klironomou, E. Kardamaki, G. K. Boulogiannis, G. E. Katsoprinakis, D. Sofikitis, T. P. Rakitzis, Gas-phase optical activity measurements using a compact cavity ringdown polarimeter. *Laser Phys.* **30**, 075602 (2020).
19. J. L. Hall, J. Ye, L.-S. Ma, Measurement of mirror birefringence at the sub-ppm level: Proposed application to a test of QED. *Phys. Rev. A* **62**, 13815 (2000).
20. G. Bailly, R. Thon, C. Robilliard, Highly sensitive frequency metrology for optical anisotropy measurements. *Rev. Sci. Instrum.* **81**, 033105 (2010).
21. X. Yu, Z.-P. Yao, Chiral recognition and determination of enantiomeric excess by mass spectrometry: A review. *Anal. Chim. Acta* **968**, 1–20 (2017).
22. S. M. Wilson, K. B. Wiberg, J. R. Cheeseman, M. J. Frisch, P. H. Vaccaro, Nonresonant optical activity of isolated organic molecules. *J. Phys. Chem. A* **109**, 11752–11764 (2005).
23. S. M. van Ruth, Methods for gas chromatography-olfactometry: A review. *Biomol. Eng.* **17**, 121–128 (2001).
24. L. R. Pendrill, Refractometry and gas density. *Metrologia* **41**, S40–S51 (2004).
25. N. Shukla, A. J. Gellman, Chiral metal surfaces for enantioselective processes. *Nat. Mater.* **19**, 939–945 (2020).
26. F. Tassinari, J. Steidel, S. Paltiel, C. Fontanesi, M. Lahav, Y. Paltiel, R. Naaman, Enantioseparation by crystallization using magnetic substrates. *Chem. Sci.* **10**, 5246–5250 (2019).
27. T. K. T. Do, F. Hadji-Minaglou, S. Antoniotti, X. Fernandez, Authenticity of essential oils. *TrAC Trends Anal. Chem.* **66**, 146–157 (2015).
28. K. Sindelarova, C. Granier, I. Bouarar, A. Guenther, S. Tilmes, T. Stavrakou, J. F. Müller, U. Kuhn, P. Stefani, W. Knorr, Global data set of biogenic VOC emissions calculated by the MEGAN model over the last 30 years. *Atmos. Chem. Phys.* **14**, 9317–9341 (2014).
29. H. Zhang, L. D. Yee, B. H. Lee, M. P. Curtis, D. R. Worton, G. Isaacman-VanWertz, J. H. Offenberg, M. Lewandowski, T. E. Kleindienst, M. R. Beaver, A. L. Holder, W. A. Lonneman, K. S. Docherty, M. Jaoui, H. O. T. Pye, W. Hu, D. A. Day, P. Campuzano-Jost, J. L. Jimenez, H. Guo, R. J. Weber, J. de Gouw, A. R. Koss, E. S. Edgerton, W. Brune, C. Mohr, F. D. Lopez-Hilfiker, A. Lutz, N. M. Kreisberg, S. R. Spielman, S. V. Hering, K. R. Wilson, J. A. Thornton, A. H. Goldstein, Monoterpenes are the largest source of summertime organic aerosol in the southeastern United States. *Proc. Natl. Acad. Sci. U.S.A.* **115**, 2038–2043 (2018).
30. J. K. Holopainen, J. Gershenzon, Multiple stress factors and the emission of plant VOCs. *Trends Plant Sci.* **15**, 176–184 (2010).
31. J. Williams, Organic trace gases in the atmosphere: An overview. *Environ. Chem.* **1**, 125–136 (2004).

32. N. Zannoni, D. Leppla, P. I. L. S. de Assis, T. Hoffmann, M. Sá, M. Araújo, J. Williams, Surprising chiral composition changes over the Amazon rainforest with height, time and season. *Commun. Earth Environ.* **1**, 4 (2020).

33. T. Norin, Chiral chemodiversity and its role for biological activity. Some observations from studies on insect/insect and insect/plant relationships. *Pure Appl. Chem.* **68**, 2043–2049 (1996).

34. M. Heil, R. Karban, Explaining evolution of plant communication by airborne signals. *Trends Ecol. Evol.* **25**, 137–144 (2010).

35. J. Williams, N. Yassaa, S. Bartenbach, J. Lelieveld, Mirror image hydrocarbons from tropical and boreal forests. *Atmos. Chem. Phys.* **7**, 973–980 (2007).

36. W. Song, J. Williams, N. Yassaa, M. Martinez, J. A. A. Carnero, P. J. Hidalgo, H. Bozem, J. Lelieveld, Winter and summer characterization of biogenic enantiomeric monoterpenes and anthropogenic BTEX compounds at a Mediterranean Stone Pine forest site. *J. Atmos. Chem.* **68**, 233–250 (2011).

37. N. Yassaa, W. Song, J. Lelieveld, A. Vanhatalo, J. Bäck, J. Williams, Diel cycles of isoprenoids in the emissions of Norway spruce, four Scots pine chemotypes, and in Boreal forest ambient air during HUMPPA-COPEC-2010. *Atmos. Chem. Phys. Discuss.* **12**, 10425–10460 (2012).

38. M. Staudt, J. Byron, K. Piquemal, J. Williams, Compartment specific chiral pinene emissions identified in a Maritime pine forest. *Sci. Total Environ.* **654**, 1158–1166 (2019).

39. M. Glasius, A. H. Goldstein, Recent discoveries and future challenges in atmospheric organic chemistry. *Environ. Sci. Technol.* **50**, 2754–2764 (2016).

40. J. Fäldt, H. Solheim, B. Långström, A.-K. Borg-Karlson, Influence of fungal infection and wounding on contents and enantiomeric compositions of monoterpenes in phloem of pinus sylvestris. *J. Chem. Ecol.* **32**, 1779–1795 (2006).

41. E. Woolfenden, Monitoring VOCs in air using sorbent tubes followed by thermal desorption-capillary GC analysis: Summary of data and practical guidelines. *J. Air Waste Manage. Assoc.* **47**, 20–36 (1997).

42. R. Sheu, A. Marcotte, P. Khare, S. Charan, J. C. Ditto, D. R. Gentner, Advances in offline approaches for chemically speciated measurements of trace gas-phase organic compounds via adsorbent tubes in an integrated sampling-to-analysis system. *J. Chromatogr. A* **1575**, 80–90 (2018).

43. G. Eerdekens, N. Yassaa, V. Sinha, P. P. Aalto, H. Aufmhoff, F. Arnold, V. Fiedler, M. Kulmala, J. Williams, VOC measurements within a boreal forest during spring 2005: On the occurrence of elevated monoterpene concentrations during night time intense particle concentration events. *Atmos. Chem. Phys.* **9**, 8331–8350 (2009).

44. N. Yassaa, J. Williams, Analysis of enantiomeric and non-enantiomeric monoterpenes in plant emissions using portable dynamic air sampling/solid-phase microextraction (PDAS-SPME) and chiral gas chromatography/mass spectrometry. *Atmos. Environ.* **39**, 4875–4884 (2005).

45. R. Grote, Ü. Niinemets, Modeling volatile isoprenoid emissions—A story with split ends. *Plant Biol. (Stuttg.)* **9**, e42–e59 (2007).

46. A. Ghirardo, K. Koch, R. Taipale, I. N. A. Zimmer, J.-P. Schnitzler, J. Rinne, Determination of de novo and pool emissions of terpenes from four common boreal/alpine trees by $^{13}CO_2$ labelling and PTR-MS analysis. *Plant Cell Environ.* **33**, 781–792 (2010).

47. Ü. Niinemets, U. Kuhn, P. C. Harley, M. Staudt, A. Arneth, A. Cescatti, P. Ciccioli, L. Copolovici, C. Geron, A. Guenther, J. Kesselmeier, M. T. Lerdau, R. K. Monson, J. Peñuelas, Estimations of isoprenoid emission capacity from enclosure studies: Measurements, data processing, quality and standardized measurement protocols. *Biogeosciences* **8**, 2209–2246 (2011).

48. L. de Azevedo Marques, R. R. Catharino, R. E. Bruns, M. N. Eberlin, Electrospray ionization mass spectrometry fingerprinting of perfumes: Rapid classification and counterfeit detection. *Rapid Commun. Mass Spectrom.* **20**, 3654–3658 (2006).

49. K. Chingin, G. Gamez, H. Chen, L. Zhu, R. Zenobi, Rapid classification of perfumes by extractive electrospray ionization mass spectrometry (EESI-MS). *Rapid Commun. Mass Spectrom.* **22**, 2009–2014 (2008).

50. D. V. Savatin, G. Gramegna, V. Modesti, F. Cervone, Wounding in the plant tissue: The defense of a dangerous passage. *Front. Plant Sci.* **5**, 470 (2014).

51. I. S. Martinez, M. D. Peterson, C. J. Ebben, P. L. Hayes, P. Artaxo, S. T. Martin, F. M. Geiger, On molecular chirality within naturally occurring secondary organic aerosol particles from the central Amazon Basin. *Phys. Chem. Chem. Phys.* **13**, 12114–12122 (2011).

52. J. M. Cash, M. R. Heal, B. Langford, J. Drewer, A review of stereochemical implications in the generation of secondary organic aerosol from isoprene oxidation. *Environ Sci Process Impacts* **18**, 1369–1380 (2016).

53. A. Bellcross, A. G. Bé, F. M. Geiger, R. J. Thomson, Molecular chirality and cloud activation potentials of dimeric α-pinene oxidation products. *J. Am. Chem. Soc.* **143**, 16653–16662 (2021).

54. A. Gray Bé, M. A. Upshur, P. Liu, S. T. Martin, F. M. Geiger, R. J. Thomson, Cloud activation potentials for atmospheric α-pinene and β-caryophyllene ozonolysis products. *ACS Cent. Sci.* **3**, 715–725 (2017).

55. W. H.-P. Thiemann, U. Meierhenrich, ESA mission ROSETTA will probe for chirality of cometary amino acids. *Orig. Life Evol. Biosph.* **31**, 199–210 (2001).

56. S. Droulias, L. Bougas, Surface plasmon platform for angle-resolved chiral sensing. *ACS Photonics* **6**, 1485–1492 (2019).

57. S. Droulias, L. Bougas, Absolute chiral sensing in dielectric metasurfaces using signal reversals. *Nano Lett.* **20**, 5960–5966 (2020).

58. J. C. Visschers, O. Tretiak, D. Budker, L. Bougas, Continuous-wave cavity ring-down polarimetry. *J. Chem. Phys.* **152**, 164202 (2020).